3-2011

Analysis of Interband, Intraband, and Plasmon Polariton Transitions in Silver Nanoparticle Films Via In Situ Real-Time Spectroscopic Ellipsometry

S. A. Little

R. W. Collins

S. Marsillac
Old Dominion University, Smarsill@odu.edu

Original Publication Citation

Little, S.A., Collins, R.W., & Marsillac, S. (2011). Analysis of interband, intraband, and plasmon polariton transitions in silver nanoparticle films via *in situ* real-time spectroscopic ellipsometry. *Applied Physics Letters, 98*(101910), 1-3. doi: 10.1063/1.3564894

AIP | Applied Physics Letters

Analysis of interband, intraband, and plasmon polariton transitions in silver nanoparticle films via in situ real-time spectroscopic ellipsometry

S. A. Little, R. W. Collins, and S. Marsillac

Citation: Applied Physics Letters **98**, 101910 (2011); doi: 10.1063/1.3564894
View online: http://dx.doi.org/10.1063/1.3564894
View Table of Contents: http://scitation.aip.org/content/aip/journal/apl/98/10?ver=pdfcov
Published by the AIP Publishing

Analysis of interband, intraband, and plasmon polariton transitions in silver nanoparticle films via *in situ* real-time spectroscopic ellipsometry

S. A. Little, R. W. Collins, and S. Marsillac[a)]
Center for Photovoltaics Innovation and Commercialization (PVIC), University of Toledo, Toledo, Ohio 43606, USA

(Received 10 September 2010; accepted 20 February 2011; published online 10 March 2011)

The dielectric function of Ag nanoparticle films, deduced from an analysis of *in situ* real-time spectroscopic ellipsometry (RTSE) measurements, is found to evolve with time during deposition in close consistency with the film structure, deduced in the same RTSE analysis. In the nucleation regime, the intraband dielectric function component is absent and plasmon polariton behavior dominates. Only at nuclei contact, does the intraband amplitude appear, increasing above zero. Both intraband and plasmon amplitudes coexist during surface smoothening associated with coalescence. The intraband relaxation time increases rapidly after surface smoothening is complete, also in consistency with the thin film structural evolution. © *2011 American Institute of Physics*.
[doi:10.1063/1.3564894]

Resonant oscillations associated with conduction electrons in metal thin films, known collectively as surface plasmons, can couple to incident electromagnetic waves when surface structures such as roughness protrusions, gratings, or nanoparticles exist.[1] Resonance characteristics depend on electrodynamic interactions with the electrons, the surrounding polarizable media, and the relationship of the optical wavelength to the Fourier spectrum of the metallic surface profile. Thus, surface engineering permits tunable optical properties.[2] Devices utilizing such technology include sensors for biological materials[3] and those based on surface enhanced Raman spectroscopy.[4] Back contact reflectors in thin film solar cells also exhibit surface plasmonic effects that influence their performance.[5]

The first *in situ* real time spectroscopic ellipsometry (RTSE) studies of metal film nucleation and growth focused on Al and Ag films.[6,7] More recently, Oates *et al.*[8] have studied the growth of Ag *in situ* over the photon energy range of 1.25–3.33 eV. In the present article, RTSE measurements spanning the range of 0.75–6.50 eV are described in detail for a Ag nanoparticle film. This broader spectral range enables a separation among the contributions due to intraband transitions at low energies, nanoparticle plasmon polariton transitions at intermediate energies, and interband transitions at high energies. It also enables the determination of thicknesses associated with the nucleating nanoparticle layer, the coalesced bulk layer, and its overlying surface roughness layer, which can then be correlated with the behavior of the dielectric function components associated with the nucleating and bulk layers.

Thin film Ag was deposited by dc magnetron sputtering onto a Si (100) wafer with a 39 nm thermal oxide using a Ag target (99.99%) in high purity Ar (99.998%). The substrate was held at room temperature, and an Ar pressure of 4 mTorr and a target power of 10 W were maintained. RTSE data were acquired *in situ* during film growth using a rotating-compensator multichannel ellipsometer with a photon energy range of 0.75–6.50 eV and a 65° incidence angle. Pairs of (Ψ,Δ) spectra were collected with a 3 s acquisition time. The optical model, including thicknesses of a bulk layer, d_b, and a surface roughness (or nucleating) layer, d_s, along with the fully characterized substrate, was used in fits to real time (Ψ,Δ) spectra by least-squares regression. The dielectric functions of the nucleating and bulk layers were parameterized whereas that of the surface roughness layer was determined from the Bruggeman effective medium theory (EMT) as a 0.5/0.5 volume fraction mixture of underlying bulk layer material and void.[9]

The imaginary parts, ε_2, of the dielectric functions for selected deposition times are shown in Fig. 1. Three spectral regions can be parameterized through the following equation:

$$\varepsilon(E) = \varepsilon_\infty + \frac{-A_D{}^2}{E^2 + i\Gamma_D E} + \frac{A_L{}^2}{E_L{}^2 - E^2 - i\Gamma_L E} + G(E), \qquad (1)$$

where

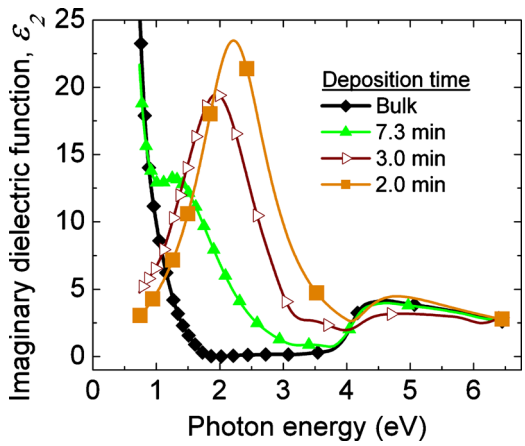

FIG. 1. (Color online) Imaginary part of the complex dielectric function ε_2 plotted as a function of photon energy for bulk Ag and for Ag obtained at selected deposition times.

[a)]Author to whom correspondence should be addressed. Electronic mail: sylvain.marsillac@utoledo.edu.

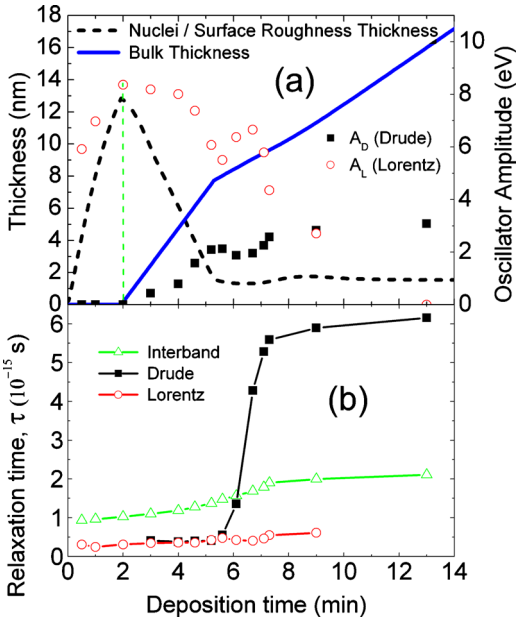

FIG. 2. (Color online) (a) Layer thicknesses and amplitudes of Drude and Lorentz components and (b) relaxation times for the intraband (Drude), nanoparticle plasmon polariton (Lorentz), and interband transitions as functions of the deposition time for a Ag thin film from nucleation though coalescence to bulk film growth.

$$G(E) = A_G(\Gamma_G/2)^{-\mu}[e^{i\phi}(E_G - E - i\Gamma_G/2)^{\mu} + e^{-i\phi}(E_G + E + i\Gamma_G/2)^{\mu}]. \quad (2)$$

At low energies, the rapid decrease in ε_2 with increasing photon energy observed at longer deposition times is attributed to free electron or intraband transitions and was fit using a Drude expression in Eq. (1) with amplitude A_D and broadening Γ_D as adjustable parameters. In the midrange energies, a well-defined peak is observed for all times in Fig. 1, which shifts to lower energies with increasing time and merges with the intraband transitions. This peak is associated with nanoparticle plasmon polariton transitions and is modeled using a Lorentz oscillator expression in Eq. (1) with amplitude A_L, resonance energy E_L, and broadening Γ_L, as adjustable parameters.[7] At high energies, the absorption step observed for all times is attributed to the onset of interband transitions originating from the d-bands and was modeled using the more general critical point oscillator expression provided in Eq. (2).[10,11] The free parameters in this case include the amplitude A_G, band gap energy E_G, broadening Γ_G, phase ϕ, and exponent μ.

Figure 2(a) shows the evolution of the nucleating, bulk, and surface roughness layer thicknesses with time. Three stages are clearly identified in the growth process.[6,12] In the first stage after opening the shutter ($t=0$ min), the Ag film nucleates following a Volmer–Weber growth mode, evidenced by an abrupt increase in d_s with no detectable increase in d_b. In the second stage starting at $t=2$ min, the enlarging nanoparticle nuclei have made contact and generate a well-defined d_b value (i.e., greater than a monolayer in thickness). In this stage, the nucleating layer is replaced by a top-most surface roughness layer whose thickness is found to decrease rapidly with bulk layer thickness as the nuclei coalesce into d_b. As a result, the d_b growth rate is larger during coalescence than in steady state. In the third stage ($t > 5$ min), d_s has saturated at a nearly constant value while d_b grows at a constant steady-state rate until the shutter is closed. The final film thickness from RTSE agrees well (to within 10%) with that from profilometry. The root mean square surface roughness thickness, d_{AFM}, measured from tapping mode atomic force microscopy (AFM) at the end of the deposition was ~1 nm, which compares with the final RTSE value of $d_s = 1.6$ nm. This yields the relationship $d_s \sim 1.6 d_{AFM}$, which is close to that observed for silicon thin films.[13]

Also shown in Fig. 2(a) is the Drude component amplitude A_D and Lorentz oscillator amplitude A_L as functions of time for comparison with the structural evolution. At the deposition onset, A_L increases as the nucleating layer thickness increases due to the increase in the volume fraction of nanoparticles. During this first stage, A_D is not detectable due to the absence of pathways for free electron conduction in the nucleating film. At the vertical dashed line ($t=2$ min), however, A_L reaches its maximum just as A_D increases above zero. Thus, the vertical dashed line denotes the onset of conducting electron behavior, which simultaneously corresponds to the onset of a well-defined d_b value in a two-layer analysis. Similarly, the decrease in the Lorentz oscillator amplitude at the onset of A_D indicates that the nanoparticles that confine electrons are integrated into the conducting film structure. Thus, this stage is associated with coalescence which simultaneously corresponds to surface smoothening as seen in d_s from Fig. 2(a). This close correspondence between the structural and optical properties provides support for the validity of the overall analysis, which uses the Bruggeman EMT to determine the optical properties of the surface roughness layer, as distinct from the bulk layer, in a two-layer model.

Although there is excellent overall consistency between the sets of properties, it is interesting that a nonzero A_L value is observed even after the surface has completely smoothened. Furthermore, the Drude amplitude A_D just after complete smoothening is considerably lower than the value obtained in the thick film limit (9 eV). A likely explanation of both effects is incomplete coalescence of crystallites and trapping of void structures within the bulk layer at the substrate interface. The trapped structure and associated plasmon feature at the substrate interface are no longer observed when the overlying film becomes opaque at the resonance energy, as occurs for $d_b > 10$ nm. Consistent with this interpretation, A_D approaches the expected bulk value for $d_b > 10$ nm, indicating a higher density in the thick film limit than in the near-interface bulk layer.

The relaxation times calculated on the basis of the relation $\tau = \hbar/\Gamma$ for different dielectric function contributions are plotted as a function of deposition time in Fig. 2(b). The relaxation time of the Lorentz oscillator τ_L corresponds to the mean free time between collisions for the electrons confined within the nanoparticles. As can be observed in Fig. 2(b), τ_L is essentially constant within the range of 0.25–0.3 fs as a function of time, even as the thickness associated with the nuclei increases from 7.5 to 12.5 nm. This increase in nucleating layer thickness reflects an increase in the size of the nanoparticles as observed directly from AFM. As a result, it is concluded that the relaxation time is limited, not by scattering from nanoparticle surfaces but rather by scattering from defects, e.g., crystallite boundaries, internal to the nanoparticles; otherwise the relaxation time would increase

at the same rate as the thickness.[6] Even throughout coalescence, and as the proposed substrate interface resonances dominate, τ_L remains very short, also indicating dominance of defect scattering. In a theoretical analysis of the nanoparticle plasmon polariton, obtained by substituting the Drude expression into the Maxwell Garnett EMT,[7] τ_L equals the relaxation time in the Drude expression τ_D. This prediction is borne out by the results in Fig. 2(b), in which case there is an overlap between Lorentz and Drude values. Thus, the nanoparticles are formed not from bulklike Ag but rather from the defective Ag formed in the coalescence stage—which has a factor of 15 shorter relaxation time.

A dramatic increase in τ_D occurs starting at $t=5$ min, which corresponds to the completion of surface smoothening and the start of the third stage of growth, characterized by a nearly constant surface roughness thickness; see Fig. 2(a). Thus, in the coalescence process, the defective Ag nanostructure abruptly transitions to a larger grain polycrystalline film nearest the surface. The divergence of τ_D and τ_L at this time provides evidence for different structure of the Ag near the surface (τ_D) versus near the substrate interface (τ_L). In the third stage, a continuous, gradual increase in τ_D occurs and is attributed to grain coarsening with increasing thickness. In this stage, a linear increase in $(\tau_D)^{-1}$ with d_b^{-1} is observed, as might be expected if the grain size increases linearly with bulk layer thickness.[14] This evolution in grain size is corroborated by x-ray diffractometry. The relaxation time τ_D for the final film (70 min deposition) is 9.1 fs, which is to be compared with 37 fs for multicrystalline Ag.[15]

Compared to τ_L and τ_D, the interband transition relaxation time τ_G is longer in the nucleation stage. This is evident directly from Fig. 1 where the width of the interband onset is observed to be narrower than that of the plasmon polariton. For the interband transitions the initial electronic state is within the d-band, which has a weak dependence on electron wave vector k. For interband transitions arising from particulate Ag regions of the film, the static dielectric constant is low due to the spatial confinement of free electrons. This may lead to electron and hole Coulomb interaction that would significantly reduce the group speed associated with the excitation. For a given mean free path, this would account for the longer relaxation time in the early stage of growth as compared to the plasmon polariton, in which case electron travels in accordance with the Fermi speed. The more gradual increase in τ_G in the third stage of growth is likely to have the same origin as the rapid rise in τ_D, namely, the reduction in defect density and an increase in grain size.

In conclusion, this study emphasizes the close correspondence between the evolution of structural and optical behavior during metal film growth as deduced by *in situ* RTSE. Several features of significance have been identified that support the application of RTSE for detailed structural analysis. First, it is found that the amplitude of the Drude component increases above zero precisely at the transition from nucleation to bulk layer growth as identified by the transition from a one-layer to a two-layer optical model, using the Bruggeman EMT for the optical properties of the surface roughness layer. Furthermore, the amplitude of the plasmon polariton component reaches its maximum at this transition and decays beyond, supporting the interpretation of a transition from nanoparticle to film growth. Other less expected features have been observed including a plasmon polariton amplitude that extends beyond the completion of smoothening, suggesting a residual interface plasmon component. In addition, a relatively long relaxation time is observed for the interband transitions, suggesting a more localized excitation. Generally, RTSE proves to be a powerful tool for *in situ* and real time analysis of metal nanoparticle deposition with the prospect of deposition control for specific sensor functionalities.

[1]H. Raether, *Surface Plasmons on Smooth and Rough Surfaces and Gratings* (Springer, New York, 1988).
[2]T. R. Jensen, M. D. Malinsky, C. L. Haynes, and R. P. Van Duyne, J. Phys. Chem. B **104**, 10549 (2000).
[3]M. Malmqvist, Nature (London) **361**, 186 (1993).
[4]K. Kneipp, Phys. Today **60**(11), 40 (2007).
[5]L. R. Dahal, D. Sainju, J. Li, J. A. Stoke, N. J. Podraza, X. Deng, and R. W. Collins, *Proceedings of the 33rd IEEE Photovoltaics Specialists Conference* (IEEE, Piscataway NJ, 2008), pp. 1–6.
[6]H. V. Nguyen, I. An, and R. W. Collins, Phys. Rev. B **47**, 3947 (1993).
[7]R. W. Collins and A. S. Ferlauto, in *Handbook of Ellipsometry*, edited by H. G. Tompkins and E. A. Irene (William Andrew, Norwich, NY, 2005), p. 94.
[8]T. W. H. Oates and A. Mücklich, Nanotechnology **16**, 2606 (2005).
[9]H. Fujiwara, J. Koh, P. I. Rovira, and R. W. Collins, Phys. Rev. B **61**, 10832 (2000).
[10]P. G. Etchegoin, E. C. Le Ru, and M. Meyer, J. Chem. Phys. **125**, 164705 (2006).
[11]J. Leng, J. Opsal, H. Chu, M. Senko, and D. E. Aspnes, Thin Solid Films **313–314**, 132 (1998).
[12]I. An, H. V. Nguyen, N. V. Nguyen, and R. W. Collins, Phys. Rev. Lett. **65**, 2274 (1990).
[13]J. Koh, Y. Lu, C. R. Wronski, Y. Kuang, R. W. Collins, T. T. Tsong, and Y. E. Strausser, Appl. Phys. Lett. **69**, 1297 (1996).
[14]J. D. Walker, H. Khatri, V. Ranjan, Jian Li, R. W. Collins, and S. Marsillac, Appl. Phys. Lett. **94**, 141908 (2009).
[15]P. B. Johnson and R. W. Christy, Phys. Rev. B **6**, 4370 (1972).